FLOW INSTABILITY IN BAFFLED CHANNEL FLOW

Changwoo Kang and Kyung-Soo Yang
Department of Mechanical Engineering
Inha University
Incheon 402-751, Republic of Korea
(TEL) 82 32 860 7322
(FAX) 82 32 868 1716
ksyang@inha.ac.kr

ABSTRACT

Flow instability in baffled channel flow, where thin baffles are mounted on both channel walls periodically in the direction of the main flow, has been numerically investigated in a laminar range. The geometry considered here can be regarded as a simple model for finned heat exchangers. The aim of this investigation is to understand how baffle interval (L) and Reynolds number (Re) influence the flow instability. With a fixed baffle length of one quarter of channel height (H), ratios of baffle interval to channel height ($R_B=L/H$) between 1 and 4 are considered. The critical Reynolds number of the primary instability, a Hopf bifurcation from steady to a time-periodic flow, turned out to be minimal when R_B=3. For the particular case of R_B=1.456, we performed Floquet stability analysis in order to study the secondary instability through which a time-periodic two-dimensional flow bifurcates into a three-dimensional flow. The results obtained in this investigation are in good agreement with those computed from full simulations, and shed light on understanding and controlling flow characteristics in a finned heat exchanger, being quite beneficial to its design.

INTRODUCTION

Laminar-turbulent transition is often caused by flow instability, and regarded as an essential process towards fully turbulent flow. In many engineering applications, suppressing or triggering transition is widely used depending upon the desired type of flow, laminar or turbulent, required by the particular application. Therefore, understanding the process of laminar-turbulent transition is very important in flow control, and must be preceded by a study of flow instability associated with the particular geometry.

Flows in heat exchangers or turbulence enhancers are often characterized by finned channel flows. The thin plates mounted on channel walls ("baffles") play an important role in enhancing the heat transfer not only by enlarging the fluid contact area but also by destabilizing the flow field. The flow instability caused by the baffles triggers laminar-turbulent transition. Consequentially, mixing is greatly increased in the disturbed flow field, resulting in more effective heat transfer (Howes et al., 1991; Cheng and Huang, 1991).

Flow instability in a general two-dimensional (2D) flow has been well explained by a bifurcation theory (Roberts, 1994; Yang, 2000; Battaglia et al., 1997). Two different types of bifurcation are often observed in a 2D channel flow. One is Fold bifurcation where a steady solution bifurcates into another steady one, and the other is Hopf bifurcation where a steady solution bifurcates into a time-periodic solution (Roberts, 1994). In the case of baffled channel flow in which baffles are mounted on the channel walls symmetrically in the vertical direction and periodically in the streamwise direction, extensive studies were carried out both experimentally (Roberts, 1994) and numerically (Yang, 2000), and reported the characteristics of Hopf bifurcation associated with the flow configuration.

In this investigation, a parametric study is carried out in order to elucidate the effect of baffle interval on flow instability in baffled channel flow. The baffle length is fixed as H/4 as in the previous studies (Roberts, 1994; Yang, 2000). Firstly, we compute the critical Reynolds number for Hopf bifurcation for each value of L under consideration, searching for the most unstable baffled channel flow. Secondly, for the case of R_B=1.456, we perform Floquet stability analysis in order to elucidate the secondary instability associated with that particular flow configuration.

The geometric configuration of the baffled-channel is depicted in Fig. 1. The flow configuration considered here can be regarded as a model for finned heat exchangers, and the results obtained in the current parametric studies provide useful information for designing such devices.

FORMULATION AND NUMERICAL METHODS

The current investigation requires a parametric study where numerous numerical simulations must be performed with various values of baffle interval (L) and Reynolds number (Re). This kind of parametric study demands considerable amount of computing resources; the computing efforts can be significantly reduced by employing an immersed boundary method which facilitates implementing the baffles on a Cartesian grid system (Yang and Balaras, 2006). See Fig. 2.

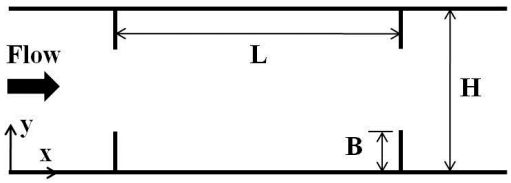

Figure 1. Flow configuration.

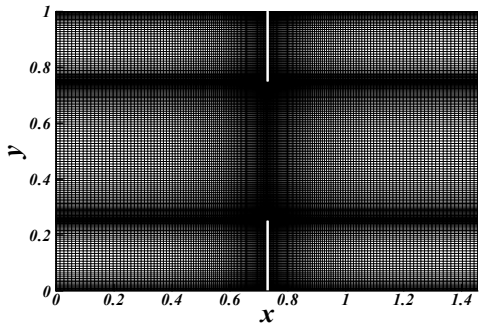

Figure 2. Grid system.

The governing equations for two-dimensional incompressible flow, modified for the immersed boundary method, are as follows;

$$\nabla \cdot \mathbf{u} = \mathbf{0} \tag{1}$$

$$\frac{\partial \mathbf{u}}{\partial t} = -\nabla \cdot (\mathbf{uu}) - \nabla p + \frac{\mathbf{1}}{\mathbf{Re}} \nabla^2 \mathbf{u} + \mathbf{f} \tag{2}$$

where $\mathbf{u}$ (or u, v), p and $\mathbf{f}$ represent velocity vector, pressure and momentum forcing, respectively. All the physical variables except p are nondimensionalized by the mean bulk velocity (U_m) and channel height (H). Pressure is nondimensionalized by a reference pressure (P_{ref}) and the dynamic pressure. Reynolds number (Re) is defined as $U_m H / \nu$, where ν is kinematic viscosity. The governing equations were discretized using a finite-volume method in a nonuniform staggered Cartesian grid system. A second-order central differencing was employed for spatial discretization of derivatives. A hybrid scheme is used for time advancement; nonlinear terms are explicitly advanced by a third-order Runge-Kutta scheme, and the other terms are implicitly advanced by the Crank-Nicolson method. A fractional step method was employed to decouple the continuity and momentum equations (Kim and Moin, 1985). The Poisson equation resulted from the second stage of the fractional step method was solved by a multigrid method. For detailed description of the numerical method used in the current investigation, See Yang and Ferziger (1993).

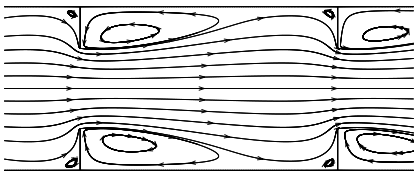

(a) Re=60

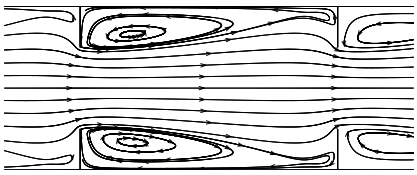

(b) Re=80

Figure 3. Streamlines of steady flow for R_B=1.456.

CHOICE OF PARAMETERS AND BOUNDARY CONDITIONS

No-slip condition is employed at all solid boundaries including the "thin" baffles of zero thickness, and the flow is assumed to be periodic in the streamwise direction (x). Therefore, we actually consider an infinitely long channel with the baffles mounted periodically in x (Fig. 1), even though the actual computational domain contains only one period in x. Simulation of unsteady streamwise-periodic flow in a channel can be classified into one of the following two cases. In one case, mass flux is fixed in time, but pressure difference between the inlet and outlet of the channel (Δp) fluctuates. In the other case, mass flux fluctuates while Δp is fixed in time. We adopted the former approach by following You et al. (2000).

The numerical resolution increases up to 256×256 ($R_B \geq 3$) computing cells in x and y directions, respectively, as Re increases. Further refinement shows less than 0.23% of difference in the growth rate of the primary instability.

RESULTS AND DISCUSSION

Onset of the Primary Instability

Streamlines of the steady symmetric solution at Re=60 and Re=80 with R_B =1.456 are shown in Fig. 3. The flow does not undergo any instability at these Reynolds numbers. At a lower Re (Fig. 3(a)), two recirculation regions are identified between the baffles; they are merged into one at a higher Re (Fig. 3(b)). Above a certain critical value of Reynolds number (Re_c), however, the flow undergoes a Hopf bifurcation leading to a solution periodic in time (Roberts, 1994). As a quantitative measure of the instability which causes the bifurcation, V_{cl} is defined as follows;

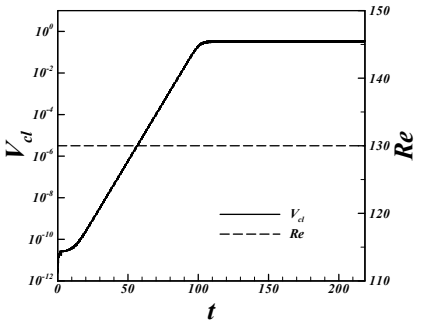

Figure 4. V_{cl} vs. time for R_B=1.456.

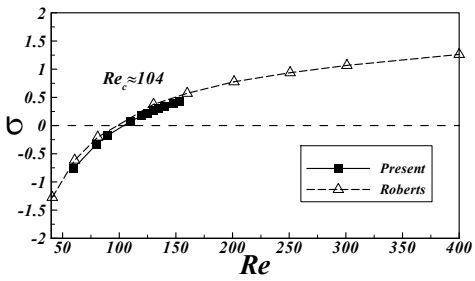

Figure 5. Instability growth rate vs. *Re* for R_B=1.456.

$$V_{cl} = \frac{1}{L}\int_0^L \left| v(x,0.5) \right| dx \qquad (3)$$

In the case of a steady solution such as in Fig. 3, the flow is symmetric in y, and obviously V_{cl} must be zero. If an instability occurs, however, the symmetry breaks up and V_{cl} grows in time. Physically, this means that the absolute flow rate through the center line increases. Therefore, V_{cl} can serve as a measure of the instability (Roberts, 1994).

Figure 4 presents the time history of V_{cl} and *Re* for R_B=1.456. The Reynolds number seems to be almost constant at *Re*=130 as intended. In the initial stage of simulation which started from low-amplitude random noise, instability does not occur. Approximately at t=13, however, a Hopf bifurcation is triggered, and V_{cl} grows exponentially afterwards, yielding the growth rate (σ) of the most unstable mode as the slope of the linear portion of the curve. Finally, nonlinearity sets in approximately at t=95, and V_{cl} periodically oscillates. The growth rates computed for various *Re* values are presented in Fig. 5; negative growth rates are obtained from the exponentially decaying V_{cl} curves. It is seen that the critical Reynolds number (Re_c) is about 104 for R_B=1.456, being in good agreement with the previous studies (Roberts, 1994; Yang, 2000). Figure 6 shows instantaneous streamlines at equal time interval for one period of flow oscillation at *Re*=130 with R_B=1.456. Vortices are generated just behind of each baffle, and travel further downstream along the channel wall to reach the next baffle. The main stream periodically

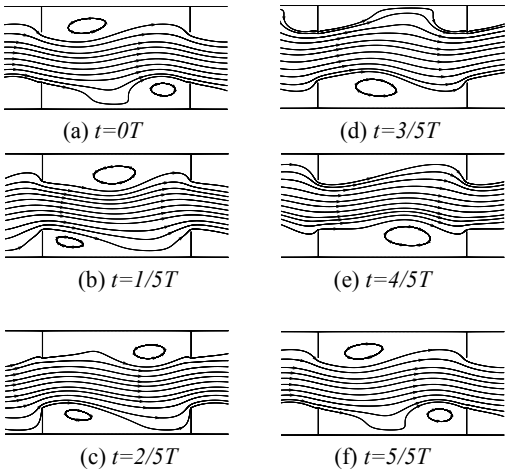

Figure 6. Streamlines of unsteady flow during one period for R_B=1.456 and *Re*=130.

moves towards the upper and lower walls in an alternating manner; the counter-rotating vortices are also shed from the tips of the upper and lower baffles, respectively, in an alternating way.

Onset of the Secondary Instability

Floquet Stability Analysis The onset of the secondary instability leading to a 3D flow can be detected by a Floquet stability analysis in which an instantaneous velocity field of the baffled channel flow is decomposed into a 2D base flow with a period T ($\mathbf{U}(x,y,t)=\mathbf{U}(x,y,t+T)$) and a 3D perturbation velocity ($\mathbf{u}'(x,y,z,t)$) as follows,

$$\mathbf{u}(x,y,z,t) = \mathbf{U}(x,y,t) + \mathbf{u}'(x,y,z,t) \qquad (4)$$

Substituting Eq. (4) into the Navier-Stokes and continuity equations, and then linearizing them, one can obtain the following governing equations for the perturbation velocity field,

$$\nabla \cdot \mathbf{u}' = \mathbf{0} \qquad (5)$$

$$\frac{\partial \mathbf{u}'}{\partial t} = -\nabla \cdot (\mathbf{u}'\mathbf{U} + \mathbf{U}\mathbf{u}') - \nabla p' + \frac{1}{Re}\nabla^2 \mathbf{u}' + \mathbf{f}' \qquad (6)$$

Here, the additional terms for the immersed boundary method are also included. No-slip condition is employed at all solid boundaries including the "thin" baffles of zero thickness ($\mathbf{u}' = \mathbf{0}$), and the perturbation velocity is assumed to be periodic in the streamwise direction (x) with a period of L. Since velocity and pressure fluctuations are assumed to be

homogeneous in the spanwise direction, they can be expressed by an inverse Fourier transform in z as follows,

$$\begin{bmatrix}\mathbf{u}'\\ p'\end{bmatrix}(x,y,z,t)=\int_{-\infty}^{\infty}\begin{bmatrix}\hat{\mathbf{u}}\\ \hat{p}\end{bmatrix}(x,y,\beta,t)e^{i\beta z}d\beta \qquad (7)$$

where $\beta=2\pi/\lambda$ represents the spanwise wave number and λ is the corresponding spanwise wavelength of a disturbance. Since Eqs. (5) and (6) are linear, modes with different $|\beta|$ can be decoupled. The governing equations for each disturbance wave are similar to Eqs. (5) and (6), except for the replacement of the gradient operator ∇ with $\nabla_\beta=(\partial/\partial x, \partial/\partial y, i\beta)$. By defining the operator $\mathbf{L}$ so that $\mathbf{L}(\hat{\mathbf{u}})$ is the right-hand side of the linearized equation, the governing equation can be written symbolically as $\frac{\partial\hat{\mathbf{u}}}{\partial t}=\mathbf{L}(\hat{\mathbf{u}})$. The general solution of this equation can be expressed as a sum of solutions of the form, $\tilde{\mathbf{u}}(x,y,\beta,t)\exp(\sigma t)$, where σ is the Floquet exponent and each Floquet mode $\tilde{\mathbf{u}}$ is a time-periodic function. Instability of the base flow $\mathbf{U}$ is determined by the Floquet multipliers, $\mu\equiv\exp(\sigma T)$; $|\mu|>1$ indicates exponentially growing perturbation. The Floquet multipliers can be obtained from the eigenvalues of $\mathbf{L}$; $\tilde{\mathbf{u}}$ represents the corresponding eigenfunctions. Recently, a one-dimensional (1D) power-type method was introduced by Robichaux et al. (1999) to estimate the maximum magnitude of the Floquet multipliers by computing the following ratio

$$|\mu|_{\max}\approx N(t+T)/N(t) \qquad (8)$$

where $N(t)$ is the L_2 norm of the perturbation velocity at an instant of time. This method was verified by Blackburn and Lopez (2003). In this study, we use the method of Robichaux et al. (1999) in conjunction with an immersed boundary method to calculate the Floquet instability of the baffled channel flow (Yoon et al., 2010). For the sake of convenience, the term "Floquet multiplier" implies the one that has the maximum magnitude among the Floquet multipliers from now on, and the subscript, "max", is dropped.

Equations (5) and (6) were temporally and spatially discretized in the same way as for the base flow. The 2D time-periodic base flow was first computed with 192×192 in x and y directions; thirty-two snapshots were saved for one period of the flow. They were fed to Eqs. (5) and (6), being Fourier interpolated at each time step, if necessary. For the Floquet stability analysis, a numerical resolution of 192×192 in x and y directions was also used.

In this section, we fix R_B=1.456 as in the previous studies (Roberts, 1994; Yang, 2000). In Fig. 7, temporal variations of $N(t)$ and $|\mu|$ are presented for Re=120 and β=1.0. A random noise was used as a perturbation velocity field ($\mathbf{u}'$) at t=0. After an initial decay, the L_2 norm of the perturbation velocity starts to grow at $t\approx2$, and establishes a linear growth at $t\approx10$ after which the Floquet multiplier becomes constant ($|\mu|=1.30$). Since $|\mu|>1.0$, this particular mode (β=1.0) turns out to be unstable to 3D disturbance.

Variation of $|\mu|$ with β are depicted in Fig. 8 for several Reynolds numbers near Re_c=104. The dashed line represents $|\mu|=1.0$, meaning neutral stability. As Re increases, the range of unstable β becomes larger, and both the maximum value of $|\mu|$ and the corresponding value of β increase. For example, the most unstable modes are β=1.01 for Re=120 and β=1.063 for Re=130, respectively. It should be noted that there exist some unstable waves of small β (i.e. large wavelengths) even for the Reynolds numbers close to the critical Reynolds number of Hopf bifurcation. This trend was also found in some other flows with wall-mounted obstacles (Amon and Patera, 1989).

Floquet multipliers in a wider range of β are shown in Fig. 9 for Re=120, 125, and 130. In the case of Re=120, the Floquet multiplier is less than 1.0 for all β greater than 1.6, confirming that only one type of unstable mode (hereafter called 'mode A') can occur at a low spanwise wave number at Re=120. For a higher Re, however, another unstable mode (hereafter called 'mode B') develops in the range of $3<\beta<5$. The critical Reynolds number of mode B turned out to be 125 as seen in Fig. 9. The spanwise wave number for mode B tends to slightly decrease as Re increases. In the case of Re=130, both mode A and mode B coexist, but mode A dominates.

Another unstable mode (hereafter called 'mode C') appears in the range of $6<\beta<9$ with further increasing Re. See Fig. 10. The critical Reynolds number of mode C is found to be 148 with the corresponding β=7.71. It should be noted that mode B is dominant for Re=153, while mode C dominates in the case of Re=187. The corresponding spanwise wave numbers are 3.15 and 7.48, respectively, which are in good agreement with the previous results of Yang (2000). By using full 3D simulations, he found that the most unstable spanwise wave numbers are 3.14 for Re=153 and 7.58 for Re=187, respectively.

Floquet Modes Flow structure of the mode of a given β can be visualized with the corresponding Floquet mode. Two-dimensional basic flow is periodic with a period T ($\mathbf{U}(x,y,t)=\mathbf{U}(x,y,t+T)$), and exhibits the following RT symmetry (Reflection-Translation symmetry).

$$\begin{aligned}U(x,y,t)&=U(x,-y,t+T/2)\\ V(x,y,t)&=-V(x,-y,t+T/2)\end{aligned} \qquad (9)$$

Here, U and V are the velocity components $\mathbf{U}$ in x and y directions, respectively. Similarly, a Floquet mode also exhibits an RT symmetry. Figure 11 presents contours of the streamwise vorticity component ($\tilde{\omega}_x$) of the Floquet mode corresponding to Re=120, β=1.0 (mode A) during one time period. White and black contours represent positive and

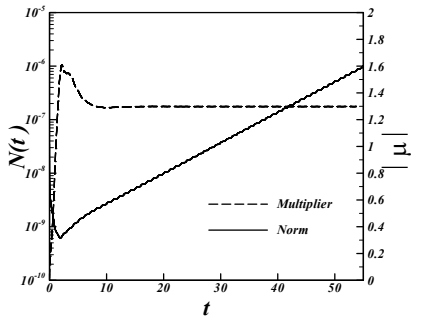

Figure 7. Growth of the norm and the Floquet multiplier for Re=120 and β=1.0.

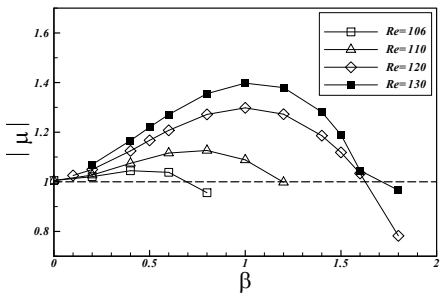

Figure 8. Variation of Floquet multipliers with spanwise wavenumber

negative values, respectively. As clearly seen in Fig. 11, $\tilde{\omega}_x$ satisfies the following odd RT symmetry.

$$\tilde{\omega}_x(x,y,t) = -\tilde{\omega}_x(x,-y,t+T/2) \tag{10}$$

The RT symmetry of $\tilde{\omega}_x$ is equivalent to the mode A of Barkley and Henderson (1996) characterized by the following relations.

$$Mode\ A: \begin{cases} \tilde{u}(x,y,t) = \tilde{u}(x,-y,t+T/2) \\ \tilde{v}(x,y,t) = -\tilde{v}(x,-y,t+T/2) \\ \tilde{w}(x,y,t) = \tilde{w}(x,-y,t+T/2) \end{cases} \tag{11}$$

In Fig. 12, are presented the contours of $\tilde{\omega}_x$ of the Floquet mode corresponding to Re=125, β=4.0 (mode B) during one time period, revealing an even RT symmetry as follows.

$$\tilde{\omega}_x(x,y,t) = \tilde{\omega}_x(x,-y,t+T/2) \tag{12}$$

The RT symmetry of $\tilde{\omega}_x$ is equivalent to the mode B of Barkley and Henderson (1996) characterized by the following relations.

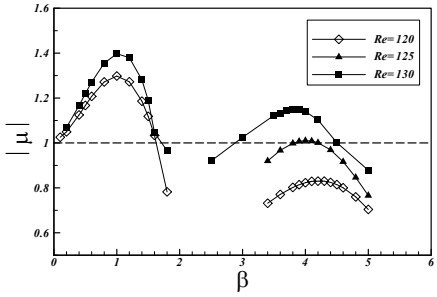

Figure 9. Variation of Floquet multipliers with spanwise wavenumber

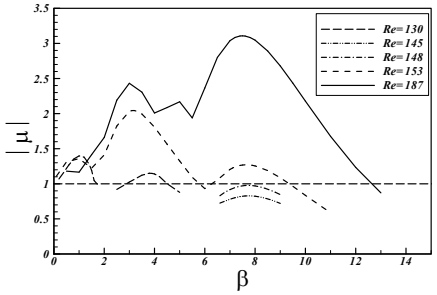

Figure 10. Variation of Floquet multipliers with spanwise wavenumber

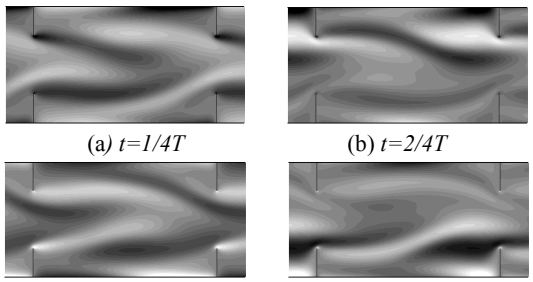

Figure 11. Contours of streamwise vorticity($\tilde{\omega}_x$) of the Floquet mode during one time period for *Re*=120 and β=1.0.

$$Mode\ B: \begin{cases} \tilde{u}(x,y,t) = -\tilde{u}(x,-y,t+T/2) \\ \tilde{v}(x,y,t) = \tilde{v}(x,-y,t+T/2) \\ \tilde{w}(x,y,t) = -\tilde{w}(x,-y,t+T/2) \end{cases} \tag{13}$$

Figure 13 shows contours of $\tilde{\omega}_x$ of the Floquet mode corresponding to Re=150, β=7.7 (mode C) during one time period, revealing the same type of RT symmetry as in the mode B.

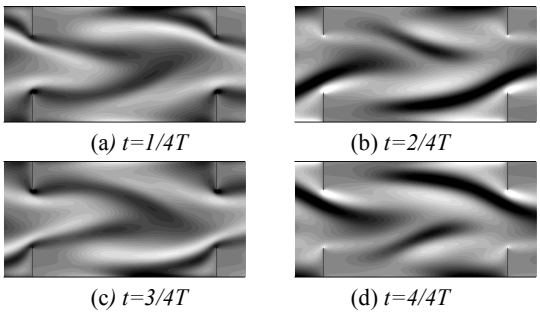

(a) *t=1/4T* (b) *t=2/4T*

(c) *t=3/4T* (d) *t=4/4T*

Figure 12. Contours of streamwise vorticity($\tilde{\omega}_x$) of the Floquet mode during one time period for *Re*=125 and β=4.0.

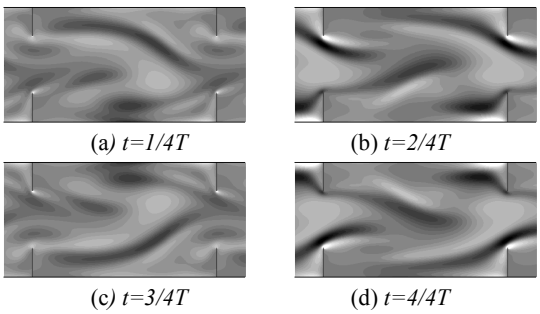

(a) *t=1/4T* (b) *t=2/4T*

(c) *t=3/4T* (d) *t=4/4T*

Figure 13. Contours of streamwise vorticity($\tilde{\omega}_x$) of the Floquet mode during one time period for *Re*=150 and β=7.7.

CONCLUSION

Flow instability in baffled channel flow, including the primary and secondary instabilities, has been numerically studied. The baffles, mounted periodically on both channel walls, are implemented on a Cartesian grid system via an immersed boundary method. The critical Reynolds number for the primary instability depends upon R_B, being minimum at R_B=3.0. Floquet stability analysis has been performed for R_B=1.456 in order to identify the most unstable spanwise mode at a given *Re*. Three dominant modes (A, B, and C) with distinct spanwise wave numbers were identified. Each mode has its own RT symmetry; odd RT symmetry for mode A, and even RT symmetry for modes B and C. The most unstable spanwise wave number obtained by the Floquet stability analysis is in good agreement with the previous result obtained by full 3D simulation. Our results shed light on complete understanding of flow instability in baffled channel flow which has great applicability in engineering.

ACKNOWLEDGMENTS

This work was supported by UVRC, Korea.

REFERENCES

Amon, C. H. and Patera, A. T., 1989, "Numerical calculation of stable three-dimensional tertiary states in grooved-channel flow", *Phys. Fluids A,* Vol. 1, pp. 2005-2009.

Barkley, D. and Henderson, R. D., 1996, "Three-dimensional Floquet stability analysis of the wake of a circular cylinder", *J. Fluid Mech.*, Vol. 322, pp. 215-241.

Battaglia, F., Tavener Simon, J., Kulkarni, A. K. and Merckle Charles, L., 1997, "Bifurcation of low Reynolds number flows in symmetric channels", *AIAA J.*, Vol. 35, pp. 99-105.

Blackburn, H. M. and Lopez, J. M., 2003, "On three-dimensional quasiperiodic Floquet instabilities of two-dimensional bluff body wakes", *Phys. Fluids*, Vol. 15, pp. L57-L60.

Cheng, C. H. and Huang, W. H., 1991, "Numerical prediction for laminar forced convection in parallel-plate channels with transverse fin arrays", *Int. J. Heat and Mass Transfer*, Vol. 34, pp. 2739-2749.

Howes, T., Mackley, M. R. and Roberts E. P. L, 1991, "The simulation of chaotic mixing and dispersion for periodic flows in baffled channels", *Chemical Engineering Science*, Vol. 46, pp.1669-1677.

Kim, J. and Moin, P., 1985, "Application of a fractional-step method to incompressible Navier-Stokes equations", *J. Comput. Phys.*, Vol. 59, pp. 308-323.

Roberts, E. P. L., 1994, "A numerical and experimental study of transition process in an obstructed channel flow", *J. Fluid Mech.*, Vol. 260, pp. 185-209.

Robichaux, J., Balachandar, S. and Vanka, S. P., 1999, "Three-dimensional Floquet instability of the wake of square cylinder", *Phys. Fluids*, Vol. 11, pp. 560-578.

Yang, J. and Balaras, E., 2006, "An embedded-boundary formulation for large-eddy simulation of turbulent flows interacting with moving boundaries", *J. Comput. Phys.*, Vol. 215, pp. 12-40.

Yang, K.-S., 2000, "Numerical investigation of instability and transition in an obstructed channel flow", *AIAA J.*, Vol. 38, pp. 1173-1178.

Yang, K.-S. and Ferziger, J. H., 1993, "Large-eddy simulation of a turbulent obstacle flow using a dynamic subgrid-scale model", *AIAA J.*, Vol. 31, pp. 1406-1413.

Yoon, D. H., Yang, K. S. and Choi, C. B., 2010, "Flow past a square cylinder with an angle of incidence", *Phys. Fluids*, Vol. 22, 043603.

You, J., Choi, H. and You, J. Y., 2000, "A modified fractional step method of keeping a constant mass flow rate in fully developed channel and pipe flows", *KSME Int. J.*, Vol. 14, pp. 547-552.